Radiation-Pattern Reconfigurable and Wideband Vector Antenna for 3-D Direction Finding

J. Duplouy[1,2], C. Morlaas[1], H. Aubert[2], P. Potier[3], and P. Pouliguen[3]

[1]ENAC, TELECOM-EMA
Université de Toulouse
F-31055 Toulouse, France
E-mail: johan.duplouy@gmail.com

[2]LAAS-CNRS, MINC
Université de Toulouse
F-31400 Toulouse, France

[3]DGA
F-75509 Paris, France

Abstract

The direction-finding performance of a radiation-pattern reconfigurable and wideband vector antenna is reported. This eight-port vector antenna consisted of the arrangement of circular arrays of Vivaldi antennas. Accurate estimation of the direction of arrival of an incoming vertically- or horizontally-polarized electromagnetic field across the three-dimensional upper half-space was achieved over a frequency bandwidth of 8.2:1 thanks to radiation-pattern reconfigurability. The proposed vector antenna offered the opportunity of using more radiation patterns than those commonly used in standard vector antennas for estimating the direction of arrival of incoming electromagnetic fields, which led to better estimation accuracy. Measurement results were found to be in good agreement with the simulated results obtained from full-wave electromagnetic simulations.

1. Introduction

Direction finding (DF) aims to estimate the direction-of-arrival (DoA) of incoming electromagnetic (EM) fields. This estimation is nowadays increasingly needed in numerous civil and military applications, such as navigation, electronic warfare, object tracking, search and rescue, and radio astronomy [1]. The latest technical inquiries for these applications are approaching the characteristics of the ideal direction finder, which are the direction of arrival estimation of incoming EM fields over the three-dimensional space (i.e., 360° of azimuth and 180° of elevation), considering their polarizations and within a wide frequency range thanks to a low-profile and compact antenna. However, most of the commercially available (see, e.g., [2-4]) or published (see, e.g., [5-6]) direction-finding antennas operate in the VHF or UHF band and offer only a two-dimensional angular coverage (i.e., only the azimuth angle of the direction of arrival can be estimated for a restricted range of elevation angles of directions of arrival). The direction-of-arrival estimation generally relies on the spatial diversity of the antenna array [7], and cannot be straightforwardly applied to design wideband direction-finding antennas targeting a three-dimensional angular coverage. Such coverage can be obtained by using an innovative direction-finding technique that allows the direction-of-arrival derivation from the measurement of the different components of the incoming EM field (ideally, the six Cartesian components, E_x, E_y, E_z, H_x, H_y, and H_z), thanks to a vector antenna (VA) [8]. Vector antennas are multi-port antennas composed of three electric dipoles and three magnetic dipoles, all spatially collocated with orthogonal orientations. Each component of the incoming EM field is hence measured through the radiation pattern (RP) of the relevant dipole. These are gaining prominence nowadays since a single vector antenna is sufficient to estimate the direction of arrival of an incoming EM field over the three-dimensional space regardless of its polarization, and notably allows compactness by substituting for a large antenna array. First, attention was mainly focused on the implementation of wideband and active vector-antenna structures [9, 10]. Second, a passive and dual-band vector antenna operating at GSM frequencies that allowed only the direction-of-arrival estimation of vertically-polarized EM fields was proposed in [11]. Fully passive vector antennas do not suffer from the intrinsic and strong limitations of active antennas, but the wideband coverage was very challenging to achieve. Recently, the authors reported first a passive, wideband and radiation-pattern reconfigurable vector antenna [12, 13]. The prototype of this vector

Figure 1a. A photograph of the Four Season vector antenna prototype (from [14]).

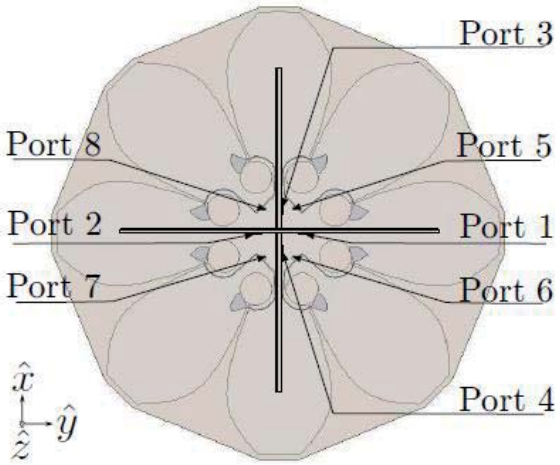

Figure 1b. The numbering of the ports of the Four Season vector antenna (from [14]).

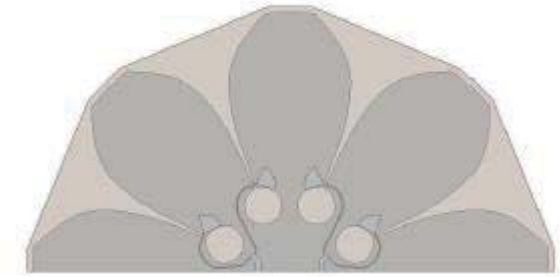

Figure 1c. The Four Season vector antenna vertical array and feeding circuit (from [14]).

antenna was only able to estimate the direction of arrival of vertically-polarized EM fields over an impedance bandwidth of 1.69:1 (or 2.10 GHz to 3.55 GHz), since only three components could be measured (E_z , H_x , and H_y). In [13], a new direction-finding technique was also proposed for radiation-pattern-reconfigurable vector antennas in order to enhance their direction-finding performance across the overall frequency bandwidth. This technique consisted of selecting and using additional radiation-pattern diversity in the direction-of-arrival estimation process. Very recently, the authors proposed the *Four Season* vector antenna [14], based on the design of the vector antenna reported in [12, 13]. A preliminary evaluation of the direction-finding performance was performed and demonstrated that this vector antenna enables the estimation of the direction of arrival of incoming vertically and horizontally polarized EM fields in the three-dimensional upper half-space over a wider bandwidth (7:1 or 1 GHz to 7 GHz).

In this article, the direction-finding performance of the Four Season vector antenna is evaluated in detail, including the evaluation of the prototype's sensitivity for direction-of-arrival estimation errors below 5° in the three-dimensional upper half-space. Moreover, the simulated and measured direction-finding performance is assessed using the new direction-finding technique proposed by the authors in [13], and compared with the preliminary performance reported in [14] (obtained without using this technique). The direction-finding performance evaluation shows the benefits of this technique.

The paper is organized as follows. The key characteristics of the Four Season vector antenna are summarized in Section 2. The selection of the additional radiation-pattern diversity to be used in the direction-of-arrival estimation process is reported in Section 3. The evaluation of direction-finding performance is investigated in Section 4. The conclusion and future directions are given in Section 5.

2. The Four Season Vector Antenna

In this section, the main characteristics of the passive, wideband, and radiation-pattern reconfigurable Four Season vector antenna, recently reported by the authors [14], are summarized (see Figure 1). The topology of this vector antenna can be divided into two parts. The vertical part consists of two spatially collocated and orthogonally oriented dual-port semi-circular arrays of four Vivaldi antennas. The horizontal part consists of a circular array of eight Vivaldi antennas. As shown in Figure 1, each port is associated with two Vivaldi antennas. Therefore, this vector antenna has a total of eight ports: four ports (ports numbers from 1 to 4) are associated with the vertical part, and four ports (ports numbers from 5 to 8) are associated with horizontal part. The vertical part enables the measurement of three components of the incoming EM field (namely, E_z , H_x , and H_y), while the horizontal part permits the measurement of the other three components (namely, H_z , E_x , and E_y). Each of these two triplets respectively allows the estimation of the direction of arrival of a vertically or

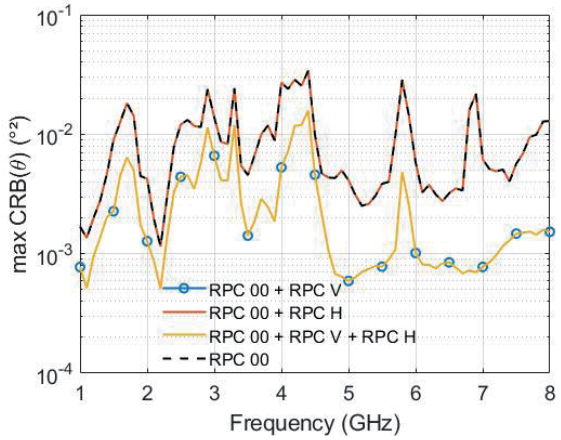

Figure 2a. The highest simulated Cramer-Rao bound (θ) of the Four Season vector antenna for an incoming vertically-polarized EM field obtained using different RPCs added to RPC 00.

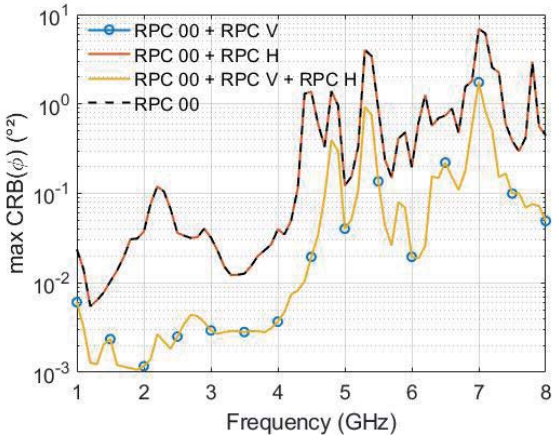

Figure 2b. The highest simulated Cramer-Rao bound (ϕ) of the Four Season vector antenna for an incoming vertically-polarized EM field obtained using different RPCs added to RPC 00.

horizontally polarized incoming EM field. Following [13] and [14], the measurements of the EM field components are derived from six sets of weighting coefficients assigned to the received signals thanks to the ability to reconfigure the radiation pattern of the Four Season vector antenna. These sets of weighting coefficients are given in Table 1, and are denoted by the acronym RPC 00 (Radiation Patterns Combination). The constitutive radiating elements exhibited a measured bandwidth of 6.77:1 (for a VSWR ≤ 2.3) between 1.24 GHz and 8.40 GHz. The antenna was included in a half-sphere within a 0.47λ radius, where λ is the free-space wavelength at 1.24 GHz. The electrical performance in terms of impedance matching and radiation-pattern properties of the Four Season vector antenna were measured in an anechoic chamber, and results were available in [14]. They were in good agreement with the data obtained from full-wave EM simulations (*HFSS* software).

Table 1. The set of weighting coefficients assigned to the signal received by the eight-port Four Season vector antenna for measuring the six components of an incoming EM field.

RPC 00	Port Number							
	1	2	3	4	5	6	7	8
E_x	0	0	0	0	1	–1	–1	1
E_y	0	0	0	0	1	1	–1	–1
E_z	1	1	1	1	0	0	0	0
H_x	1	–1	0	0	0	0	0	0
H_y	0	0	1	–1	0	0	0	0
H_z	0	0	0	0	1	–1	1	–1

3. Selection of Additional Radiation Patterns to be Used in the Direction-Finding Process

In this section, we select more sets of weighting coefficients (or accordingly, more radiation patterns) to be used in addition to RPC 00 in the direction-finding process in order to enhance the accuracy of the direction-of-arrival estimation provided by the Four Season vector antenna. These radiation patterns were chosen from an innovative method proposed by the authors in [13], which was based on the Cramer-Rao bound (CRB). The main advantage of this method is the independence regarding the direction-of-arrival estimation technique used for evaluating the direction-finding performance of the vector antenna. The objective of this method consists of selecting the additional RPC (defined as different sets of weighting coefficients providing the same radiation pattern with a rotation of 90° in the azimuthal plane) that maximizes the estimation accuracy across the entire frequency bandwidth. More specifically, the proposed method consists of choosing between several RPCs, the RPC that provides the smallest Cramer-Rao bound (in azimuth and elevation) when added to RPC 00. As in [13], we limited the possible values for the weighting coefficients β_i to $\{1, 0, -1\}$ $(i \in [1;8])$. 3^8 sets of weighting coefficients $[\beta_1, \beta_2, \beta_3, \beta_4, \beta_5, \beta_6, \beta_7, \beta_8]$ are available and could be assigned to the signals received by the eight-port antenna. Among these 6561 sets, we considered only the sets of the form $[\beta_1, \beta_2, \beta_3, \beta_4, 0, 0, 0, 0]$ and $[0, 0, 0, 0, \beta_5, \beta_6, \beta_7, \beta_8]$ in order to simplify the RPC selection. The vertical and horizontal parts of the Four Season vector antenna were therefore independently considered in order to respectively improve the direction-of-arrival estimation for vertically and horizontally polarized incoming EM fields. Consequently, two kinds of RPCs (RPC V and RPC H) were selected, one for each polarization. According to this independency, there were only 2 × 34 sets to investigate, which yielded

	Port Number							
	1	2	3	4	5	6	7	8
RPC V	1	1	1	–1	0	0	0	0
	–1	1	1	1	0	0	0	0
	1	–1	1	1	0	0	0	0
	1	1	1	–1	0	0	0	0
RPC H	0	0	0	0	1	1	1	–1
	0	0	0	0	–1	1	1	1
	0	0	0	0	1	–1	1	1
	0	0	0	0	1	1	1	–1

Table 2. Selected RPC V and RPC H with their associated set of weighting coefficients.

a total of 2 × 11 RPCs. For the sake of brevity, the sets of weighting coefficients of the tested RPCs associated with the vertical and horizontal part of the vector antennas are not written here. Only the additional weighting coefficients of the selected RPC V and RPC H are reported in Table 2. For both polarizations of the incoming EM field, the Cramer-Rao bound on θ and ϕ was computed using the parameters of [13] for the 22 RPCs, except that the study was performed from 1 GHz to 8 GHz with a 0.1 GHz frequency step. For the sake of readability, Figures 2 and 3 show only the RPCs that ensure the highest precision across the overall bandwidth and for both polarizations. The Cramer-Rao bound obtained from using only RPC 00 are also set out for comparison purposes. Globally, RPC V was more effective than RPC H for enhancing the direction-finding performance. Moreover, it can be noted that RPC H was completely inefficient in improving the direction-finding accuracy when the incoming EM field was vertically polarized. However, it can be observed that the use of both RPC V and RPC H in addition to RPC 00 slightly improved the direction-finding performance. Nonetheless, the estimation accuracy was clearly enhanced across the entire bandwidth for both polarizations thanks to additional radiation-pattern diversity. Besides, RPC H had less impact on the Cramer-Rao bound for a horizontally-polarized EM field compared to RPC V for a vertically-polarized EM field because the estimation was already more accurate using only RPC 00 for a horizontally polarized EM field (Figure 3b) than for a vertically-polarized EM field (Figure 2b). Finally, the authors would like to point out that better direction-finding performance may be obtained by taking account of a huge amount of sets of weighting coefficients of the form $[\beta_1, \beta_2, \beta_3, \beta_4, \beta_5, \beta_6, \beta_7, \beta_8]$ and also by considering complex values for selecting the additional RPCs. However, since the resulting number of possibilities would increase, the process of selection by computing and analyzing the Cramer-Rao bound would be more time consuming.

4. Measurement of the Direction-Finding Performance of the Four Season Vector Antenna Using Additional Radiation Patterns

4.1 Measured Direction-Finding Performance Using the Additional Radiation Patterns

The accuracy of the direction-of-arrival estimation can be derived from using the Four Season vector antenna and the MUSIC (MUltiple Signal Classification) algorithm [15]. In this section, we evaluate the accuracy of the direction-of-arrival estimation of a vertically or horizontally polarized incoming EM field using the measurement of its six components (RPC 00) and additional radiation-pattern diversity (RPC V and RPC H). The scenario used for this evaluation was the same as that defined in [14]. Comparisons between full-wave EM simulations and measurements results were also carried out to validate the predicted

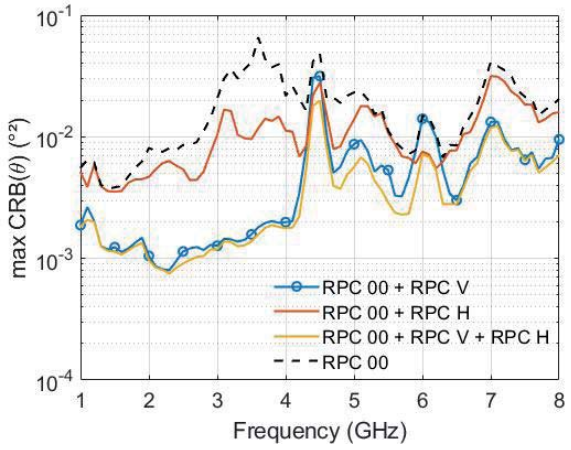

Figure 3a. The highest simulated Cramer-Rao bound (θ) of the Four Season vector antenna for an incoming horizontally-polarized EM field obtained using different RPCs added to RPC 00.

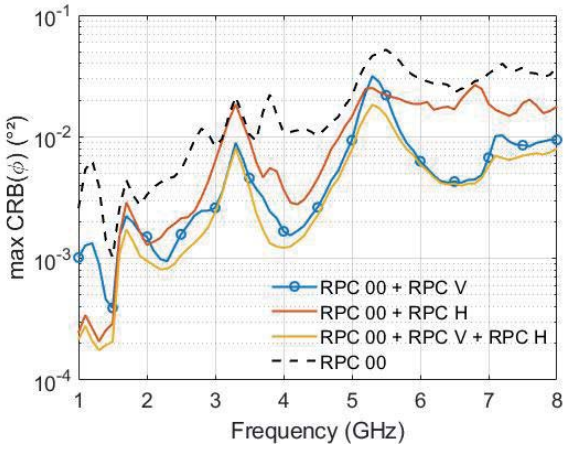

Figure 3b. The highest simulated Cramer-Rao bound (ϕ) of the Four Season vector antenna for an incoming horizontally-polarized EM field obtained using different RPCs added to RPC 00.

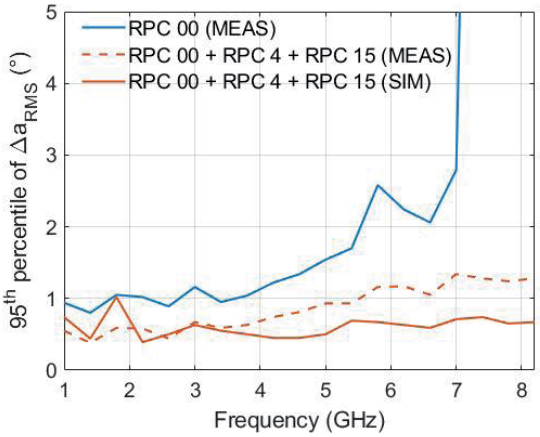

Figure 4a. The 95th percentile of Δa_{RMS} achieved with the Four Season vector antenna when additional radiation-pattern diversity is added to RPC 00 in the direction-of-arrival estimation process of an incoming vertically polarized EM field.

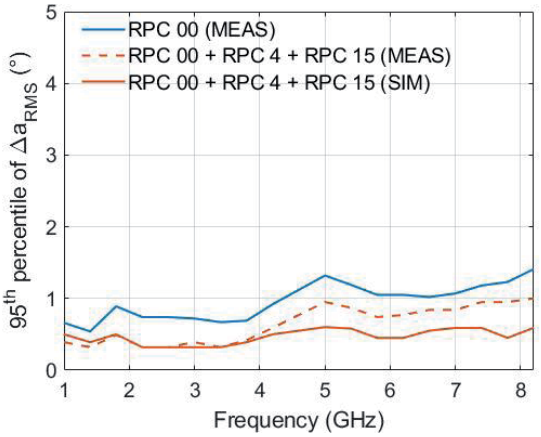

Figure 4b The 95th percentile of Δa_{RMS} achieved with the Four Season vector antenna when additional radiation-pattern diversity is added to RPC 00 in the direction-of-arrival estimation process of an incoming horizontally polarized EM field.

direction-finding performance. As in [14], the accuracy of direction-of-arrival estimation was assessed through the 95th percentile of the angular distance Δa_{RMS} (defined in Appendix A-D of [13]). Figure 4 presents the results of this investigation. The measurement results obtained in [14] when only RPC 00 were used in the direction-finding process were also recalled for comparison purposes. These correspond to the accuracy that can be achieved using only the measurement of the six components of the EM field incident upon the vector antenna. Such a measurement is theoretically sufficient to estimate its direction of arrival. In this case, the measured 95th percentile of Δa_{RMS} was smaller than 2° between 1 GHz to 5.5 GHz and exceeded 5° from 7 GHz if the incoming EM field was vertically polarized. For an incoming horizontally polarized EM field, the measured 95th percentile of Δa_{RMS} was smaller than 2° from 1 GHz to 8.2 GHz. Using additional radiation-pattern diversity, the accuracy was enhanced approximately by a factor of two for both polarizations. The benefits were even more noticeable for a vertically polarized incident EM field in the low end of the frequency range, since the measured 95th percentile of Δa_{RMS} was found to be smaller than 1° over a wider bandwidth (8.2:1 or 1 GHz to 8.2 GHz). The same level of accuracy was also achieved for a horizontally polarized incident EM field thanks to additional radiation-pattern diversity. The improvement of the direction-finding performance was predicted by the Cramer-Rao-bound analysis reported in Figures 2 and 3. It could be observed that the Cramer-Rao bound in azimuth and elevation decreased over the entire bandwidth using RPC V and H, leading to the better estimation accuracy. Globally, there was a reasonably good agreement between measurement and simulation results. The slightly discrepancy at high frequencies could be explained by the fact that the dielectric losses were considered constant in the simulation and did not increase with the frequency as in practice, which was especially disadvantageous with the low-cost substrate (FR-4) used to manufacture the antenna.

4.2 Sensitivity of the Prototype

In this section, we evaluate the sensitivity of the Four Season vector antenna prototype using the additional radiation-pattern diversity (RPC V and RPC H) in the direction-of-arrival estimation process. The sensitivity corresponds to the minimum power density (P_{sensi}) required at the antenna location (for a given noise power level P_n) to estimate the direction of arrival with a required accuracy (defined here as the 95th percentile of $\Delta a_{RMS} \leq 5°$). To evaluate the sensitivity of the prototype, the 95th percentiles of Δa_{RMS} were measured for three frequencies (1.4 GHz, 5 GHz, and 8 GHz) and for different power-densities-to-noise-ratios (PDNR, see Appendix A-A of [13] for the definition), ranging from 12 dB/m^2 to 36 dB/m^2

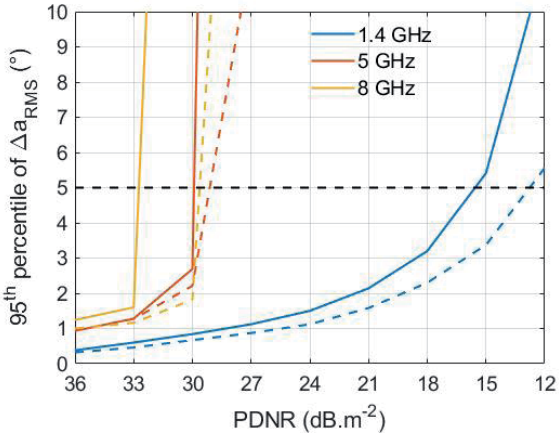

Figure 5. The measured 95th percentile of Δa_{RMS} achieved for different power-densities-to-noise-ratios and when RPC V and RPC H are added to RPC 00 in the direction-of-arrival estimation process of an incoming vertically (solid lines) or horizontally (dashed lines) polarized EM field.

Table 3. The measured sensitivity of the Four Season vector antenna using RPC 00 and RPC V and RPC H.

Frequency	P_{sensi} dBW / m^{-2}	PDNR dBW / m^{-2}
Vertical Polarization		
1.4 GHz	–125	16
5 GHz	–111	30
8 GHz	–108	33
Horizontal Polarization		
1.4 GHz	–128	13
5 GHz	–112	29
8 GHz	–111	30

(with a step of 3 dB). These frequencies corresponded approximately to the lower, central, and upper operating frequencies of the antenna. Moreover, this evaluation assumed that the incoming EM field was either vertically or horizontally polarized. Figure 5 presents the results of this analysis. For both cases, it could be seen that the sensitivity of the Four Season vector antenna was degraded as the frequency increased since the 95th percentile of Δa_{RMS} also rose. This can be explained by two main reasons. As the frequency increases, there are (1) the enhancement of the risk of angular ambiguity (defined in Appendix A-C of [13]), and (2) the decrease of the antenna's efficiency. These can lead to an increase of the estimation errors. Moreover, there is also the emergence of ripples in the radiation patterns as the frequency increases, but this phenomenon was taken into account during the evaluation of the direction-finding performance with the MUSIC algorithm through the calibration process, as detailed in [13]. It can also be noted that the sensitivity required for estimating the direction of arrival of a vertically polarized EM field for a given accuracy is higher than that of a horizontally polarized EM field. This is consistent with the Cramer-Rao bound results depicted in Figures 2 and 3, which showed that the accuracy of the elevation-angle estimation was relatively the same over the entire bandwidth for both polarizations while the azimuth-angle estimation was more accurate at higher frequencies if the incoming EM field was horizontally-polarized. To estimate the required accuracy the direction of arrival of a vertically or horizontally polarized EM field, the incoming power density required at the Four Season vector antenna location (P_{sensi}) is summarized in Table 3. From this study, the theoretical range could be easily derived for an estimation accuracy of 5°, knowing the gain and emitting power of a transmitter.

5. Conclusion

The direction-finding performance of a passive, wideband radiation-pattern reconfigurable vector antenna has been reported in this paper. The vector antenna prototype enables the accurate estimation of the direction of arrival of a vertically or horizontally polarized EM field across the three-dimensional upper half-space and over a 8.2:1 bandwidth (or 1 GHz to 8.2 GHz]) using the measurement of six EM field components and additional radiation patterns in the direction-finding process. Next steps will be focused on evaluating the direction-finding performance of this vector antenna and the benefits of the additional radiation-patterns technique in multipath and multi-source environments.

6. Acknowledgments

We would like to thank the French Defense Agency (Direction Général de l'Armement, DGA) and the Occitanie regional council for the financial support of the thesis of Johan Duplouy in the framework of the AVIAtoR3D project.

7. References

1. T. E. Tuncer and B. Friedlander, *Classical and Modern Direction-of-Arrival Estimation*, New York, Academic Press, 2009.

2. Rohde & Schwarz, "DF antenna ADD253," http://www.rohde-schwarz.com/en/product/add253, visited on June 21, 2018.

3. CRFS, "DF antenna RFeyeArray 300," https://www.crfs.com/all-products/hardware/direction-finders/array-300/, visited on June 21, 2018.

4. TCI, "DF antenna Model 643," https://www.tcibr.com/product/tci-model-643-dual-polarized-vhfuhf-dfand-spectrum-monitoring-antenna/, visited on June 21, 2018.

5. A. Bellion and C. Le Meins, "Directional Multiple-Polarization Wide Band Antenna Network," US Patent US20110133986A1, December 21, 2007.

6. L. Scorrano and L. Dinoi, "Experimental Characterization of a Dual-Polarized Direction Finding Array for VHF-UHF Frequency Bands," European Conference on Antennas and Propagation (EUCAP), March 2017, pp. 1295-1298.

7. P. Gething, *Radio Direction Finding and Superresolution*, London, P. Peregrinus Ltd., 1991.

8. A. Nehorai and E. Paldi, "Vector-Sensor Array Processing for Electromagnetic Source Localization," *IEEE Transactions on Signal Processing*, **42**, 2, February 1994, pp. 376-398.

9. B. Almog, "Compact 3D Direction Finder," Patent EP20120184835, March 20, 2013.

10. A. Musicant, B. Almog, N. Oxenfeld, and R. Shavit, "Vector Sensor Antenna Design for VHF Band," *IEEE Antennas and Wireless Propagation Letters*, **14**, 2015, pp. 1404-1407.

11. J. Lominé, C. Morlaas, C. Imbert, and H. Aubert, "Dual-Band Vector Sensor for Direction of Arrival Estimation of Incoming Electromagnetic Waves," *IEEE Transactions on Antennas and Propagation*, **63**, 8, August 2015, pp. 3662-3671.

12. J. Duplouy, C. Morlaas, H. Aubert, P. Potier, P. Pouliguen, and C. Djoma, "Reconfigurable Grounded Vector Antenna for 3-D Electromagnetic Direction-Finding Applications," *IEEE Antennas and Wireless Propagation Letters*, **17**, 2, February 2018, pp. 197-200.

13. J. Duplouy, C. Morlaas, H. Aubert, P. Potier, and P. Pouliguen," Wideband and Reconfigurable Vector Antenna Using Radiation Pattern Diversity for 3-D Direction-of-Arrival Estimation," *IEEE Transactions on Antennas and Propagation*, **67**, 6, June 2019, pp. 3586-3596.

14. J. Duplouy, C. Morlaas, H. Aubert, P. Potier, and P. Pouliguen, "Wideband Vector Antenna for Dual-Polarized and Three-Dimensional Direction-Finding Applications," *IEEE Antennas and Wireless Propagation Letters*, **18**, 8, August 2019, pp. 1572-1575.

15. R. Schmidt, "Multiple Emitter Location and Signal Parameter Estimation," *IEEE Transactions on Antennas and Propagation*, **34**, 3, March 1986, pp. 276-280.